Torque-Balanced High-Density Steady States of Single-Component Plasmas

J. R. Danielson and C. M. Surko

Department of Physics, University of California at San Diego, La Jolla, California 92093, USA

(Received 10 September 2004; published 24 January 2005)

Electron plasmas in a Penning-Malmberg trap are compressed radially using a rotating electric field (the ''rotating-wall technique''). For large electric fields, plasmas can be compressed over a broad range of frequencies. This permits access to a novel high-density regime in which outward transport is insensitive to plasma density. The limiting density occurs when the plasma rotation frequency equals the rotating-wall frequency. Characteristics of the resulting torque-balanced steady states are described, and implications for high-density electron and positron plasma confinement are discussed.

DOI: 10.1103/PhysRevLett.94.035001 PACS numbers: 52.27.Jt, 52.25.Fi, 52.55.Dy

Trapped single-component plasmas are important in many contexts, such as the confinement and tailoring of antiproton and positron plasmas for numerous applications, including atomic physics and tests of fundamental symmetries and the characterization of materials [1]. Consequently, it is important to understand the range of accessible plasma parameters, including the limits on plasma temperature, density, and confinement time. Here we explore the range of torque-balanced steady states of electron plasmas that can be achieved using cyclotron cooling to balance plasma heating and a rotating electric field [i.e., the ''rotating-wall'' (RW) technique], for radial compression and the mitigation of outward transport.

There is now a large body of knowledge regarding single-component plasmas in Penning-Malmberg traps although many questions remain [2]. The rotating-wall technique was developed to confine and compress electron [3,4] and ion plasmas [5,6] and was later used to compress positron plasmas [7], including those used for antihydrogen production [8]. It provides an effective tool to mitigate outward transport and to compress plasmas radially, across the magnetic field. With one exception [7], coupling to the plasma has been achieved by either tuning the RW frequency to a Trivelpiece-Gould (TG) mode [4] or phase locking to a strongly coupled ion crystal [6]. This Letter describes a novel, strong-drive RW regime in which efficient compression can be achieved over a broad range of frequencies *without* tuning to plasma modes.

Plasma compression is expected to be inhibited by outward transport, typically ascribed to magnetic or electrostatic asymmetries [4,9–11]. The transport rate, $\Gamma_0 = -(1/n)(dn/dt)$, is typically found to scale as $\Gamma_0 \propto n^2 L_p^2/B^2$, where n and L_p are the plasma density and length, and B is the magnetic field. In the experiments reported here, plasmas can be compressed to where Γ_0 becomes insensitive to plasma density (i.e., $\Gamma_0 \propto n^0$). This regime of reduced transport results in high plasma densities (e.g., $n \geq 10^{10}\,\mathrm{cm}^{-3}$) with moderately low plasma temperatures (i.e., in energy units, $T \lesssim 0.2$ eV). This Letter focuses on describing the range of compressed steady-state plasmas that can be created in this regime. The implications of these results for the practical limits on positron storage are also discussed.

Experiments are performed in a cylindrical Penning-Malmberg trap, shown schematically in Fig. 1. Electron plasmas are injected using a standard electron gun, with initial plasma radii $R_p \sim 1$–2 mm. Plasmas are confined radially by the magnetic field, with axial confinement provided by voltages (typically -100 V) applied to the end electrodes. The wall diameter is 2.54 cm, and the plasma length, L_p, can be varied in the range $5 \leq L_p \leq 25$ cm, using different electrode configurations.

Rotating electric fields are applied to the plasma using a special-purpose, four-phase rf generator attached to a four-segment electrode. Each segment extends 90° azimuthally and 2.54 cm axially; combined, they produce a radial electric field with azimuthal mode number $m_\theta = 1$ rotating in the same direction as the plasma.

The data presented here correspond to the RW electrode located near one end of the plasma column, as shown in Fig. 1, but good confinement and compression have also been achieved with the RW at other locations. Theoretically, an $m_\theta = 1$ dipole drive applied over the entire plasma can drive no torque [12]. Although not studied in detail, we find that good compression can be achieved as long as the axial extent of the RW electrode is less than half the plasma length.

The trap is operated in ''inject-manipulate-dump'' cycles that exhibit very good shot-to-shot reproducibility; for example, $\delta N/N \sim 1\%$, where N is the particle number.

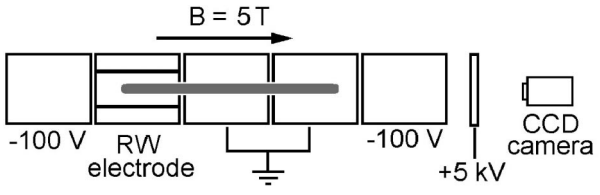

FIG. 1. Schematic diagram of the experiment (not to scale; not all electrodes are shown).

Dumped plasmas are accelerated to about +5 kV before striking a phosphor screen, with the resulting images recorded by a charge-coupled device (CCD) camera (effective pixel size = 12.5 μm in the plasma). This z-integrated profile and the trap geometry are used as the inputs to a Poisson solver to calculate the plasma length and density. For fixed N, the space charge potential, Φ, increases as the plasma is compressed, and so the plasma length changes slightly as a function of density. Typical values of Φ range from 10 to 80 V.

The parallel plasma temperature, $T_\parallel$, is measured by slowly lowering the confinement voltage and measuring the escaping charge [13]. For the plasmas studied here, the perpendicular-to-parallel equilibration rate is rapid ($\nu_{\perp\parallel} > 1000\ \mathrm{s}^{-1}$), so $T_\parallel \approx T_\perp \equiv T$ [14]. Heat transport is also rapid with a thermal relaxation time $\tau_T < 10$ ms [15], and so we assume the temperature is independent of the radius. The plasma cools by cyclotron radiation in the 5 T magnetic field at a rate $\Gamma_c = (1/T)(dT/dt) \sim 6\ \mathrm{s}^{-1}$ [14,16], which is fast compared to the compression and expansion time scales. Thus, in most cases, the plasmas remain relatively cool (i.e., $T \lesssim 0.2$ eV; $T/e\Phi \ll 1$), even in the presence of strong RW fields.

After the plasma is injected into the trap, the RW field is turned on with amplitude V_{RW} and frequency f_{RW}. The evolution of the plasma is studied by repeating the experiment for different hold times. Examples of plasma compression for $L_p \approx 14$ cm are shown in Fig. 2(a), with an applied rotating-wall voltage $V_{\mathrm{RW}} = 1$ V at four different RW frequencies. Here, the RW is on for 20 s, and then the expansion is studied after the RW is turned off. There are two data points at each time for each frequency. They typically differ by <1%, demonstrating the robust compression and reproducibility of the experiments.

As shown in Fig. 2(a), the plasma reaches a steady state after ~5 s. The limiting, steady-state density increases as the RW drive frequency is increased. Experiments on longer time scales show that this steady-state density *can be maintained* ($\Delta n/n < 5\%$) *for more than 24 h.* When the RW is turned off, the density decays exponentially at a slow rate ($< 0.1\ \mathrm{s}^{-1}$), even at the highest densities studied.

Figure 3 shows three representative radial profiles during plasma compression for $f_{\mathrm{RW}} = 6$ MHz. Other than during rapid compression, the plasma profiles are close to that of a rigid rotor (i.e., constant density), except slightly broadened at larger radii. This is likely due to large plasma viscosity at these densities and temperatures (viscous relaxation time $\tau_v < 5$ ms) [17,18].

In Fig. 4, the steady-state density is plotted for a broad range of RW frequencies for three plasma lengths. Both the density scale and a scale in units of the central $E \times B$ rotation frequency, f_E, are shown, where $f_E \equiv n_0 ec/B \approx 2.9(n/10^{10}\ \mathrm{cm}^{-3})$ MHz. The thick solid line represents $f_{\mathrm{RW}} = f_E$, namely, the density corresponding to rigid rotation at the RW frequency. The occasional "steps" in the data are discussed below. Above a minimum RW amplitude (dependent on frequency, but typically $V_{\mathrm{RW}} > 0.5$ V), strong compression is achieved over a wide range of frequencies, with no need to tune to a plasma mode. We refer to this as the strong-drive regime.

At smaller V_{RW}, compression is observed only at distinct frequencies (e.g., the solid points in Fig. 4), consistent with previous experiments [4]. However, those experiments were done at $B = 4$ T with 7 times larger transport rate. It is likely that the reduced cyclotron cooling and larger outward transport inhibited observation of the strong-drive regime reported here.

The data in Fig. 4 illustrate a key result, namely, that, in the strong-drive regime, the effect of the RW is to increase plasma density until the plasma rotation frequency is, to within experimental accuracy, that of the RW. The fact that the compression ceases at this value of f_{RW} is consistent with thermodynamic arguments [12]. Further, as shown in Fig. 2(b), if f_{RW} is abruptly changed after compression to a steady state, the plasma quickly expands or compresses to the new steady-state density corresponding to this value of f_{RW}.

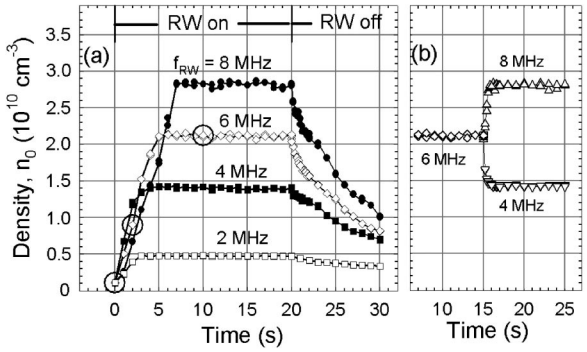

FIG. 2. (a) Central density, n_0, vs time during rotating-wall compression for four different drive frequencies. All cases have $N \sim 5.6 \times 10^8$, $V_{\mathrm{RW}} = 1.0$ V, and $Lp \approx 14$ cm. (b) Rapid response to an abrupt change in drive frequency: from 6 to 8 MHz (△), and to 4 MHz (▽).

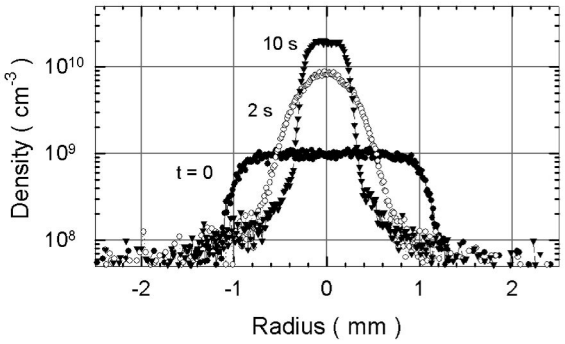

FIG. 3. Three representative profiles during plasma compression for the conditions of Fig. 2, with $f_{\mathrm{RW}} = 6$ MHz, at the times marked by ○ in Fig. 2.

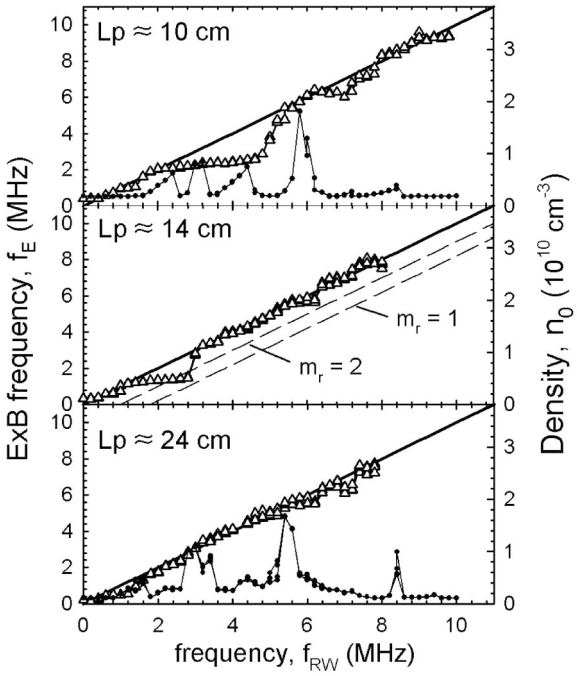

FIG. 4. Steady-state density vs applied RW frequency for three plasma lengths with $N \sim 4.5 \times 10^8$ electrons: (△) $V_{\mathrm{RW}} = 1.0$ V, demonstrating strong-drive compression at all frequencies; and (●) $V_{\mathrm{RW}} = 0.1$ V for 30 s, showing significant compression only at discrete frequencies. The solid lines correspond to $f_E = f_{\mathrm{RW}}$, and the dashed lines show the expected density if the RW frequency matched an $m_\theta = 1$ TG mode.

These torque-balanced equilibria are, within limits, not strongly dependent on the RW amplitude. For example, a factor of 2 decrease in amplitude (1 to 0.5 V) results in less than 10% decrease in the steady-state density.

A density limit is observed at $n_0 \sim 3 \times 10^{10}$ cm^{-3} ($f_{\mathrm{RW}} \sim 10$ MHz). At higher values of f_{RW}, it becomes difficult to compress the plasma, even though $n_0 \sim (2.4 \times 10^{-4}) n_B$, where n_B is the Brillouin density limit. There is evidence that this is not an intrinsic limit but the result of transmission-line effects in the rotating-wall circuit, leading to unbalanced drive of the segmented electrodes and excess plasma heating.

The fact that good compression can be achieved over a wide range of frequencies and that the plasma evolves smoothly to a new density limit following an abrupt change in f_{RW} indicates that RW coupling to the plasma is independent of the low-order TG modes. To within the uncertainty of the data (±5%), and ignoring the "steps," the strong-drive data in Fig. 4 correspond to $f_E \approx f_{\mathrm{RW}}$. If the coupling involved TG modes, it would be expected that $m_\theta f_E = f_{\mathrm{RW}} - f_p k_z R_p / j_{m_\theta m_r}$, with f_p the plasma frequency, $k_z \approx \pi / L_p$, and $j_{m_\theta m_r}$ is the zero of a Bessel function (see Ref. [4]). The dashed lines in Fig. 4 indicate the steady-state density expected in this case for $m_\theta = 1$, and $m_r = 1, 2$. While we cannot rule out the possibility that the RW drives higher order modes, we have no evidence that this is the case.

Shown in Fig. 5 is the expansion rate, Γ_0, as a function of plasma density for two different plasma lengths after the RW is turned off. As discussed above, Γ_0 is typically found to have a strong dependence on n and L_p. This dependence has been written in terms of the "rigidity," $R \equiv f_b / f_E$, in the form $\Gamma_0 \propto R^{-2} \propto n^2 L^2$ [9,10], where $f_b = \bar{v}/2L_p$ is the particle bounce frequency, with $\bar{v} = \sqrt{T/m}$ the electron thermal velocity.

The dashed lines in Fig. 5 correspond to a transport rate $\Gamma_0 \approx 1.0\ \mathrm{s}^{-1} (n/10^{10}\ \mathrm{cm}^{-3})^2 (L/24\ \mathrm{cm})^2$. This is consistent with the best confinement observed in similar electron plasma experiments [4]. At lower densities, Γ_0 increases as the square of the density in accord with this scaling. At higher densities, Γ_0 approaches a maximum and becomes independent of density. Empirically, this occurs approximately at the point (vertical arrows) at which the collision frequency $\nu_{ee} = 3 f_b$ for these cold plasmas (i.e., $T \sim 0.05$ eV with the RW off). When the plasma is highly collisional, the time for a resonant interaction and trapped-particle lifetimes is reduced, and so it is plausible that this will reduce the transport [4].

When the RW is turned off, the plasma expands slowly while maintaining an approximate rigid-rotor profile. The exception is very early times (e.g., $\Delta t < 1$ s) where the central density often drops more rapidly than elsewhere in the plasma. This may reflect the fact that these RW-compressed, steady-state plasmas are not true thermal equilibria, and that in steady state, the RW continues to couple to the central portion of the plasma, even though $f_{\mathrm{RW}} \approx f_E$. It is likely that a theory of these steady states will require taking into consideration the radial dependences of the RW torque, the viscous relaxation, and the asymmetry-induced drag on the plasma.

For the data shown in Fig. 2, we can estimate the minimum RW heating rate, assuming the RW torque, $\mathcal{T}_{\mathrm{RW}}$, is that required to balance the drag on the plasma measured immediately after the RW is turned off. The heating power will then be [19]

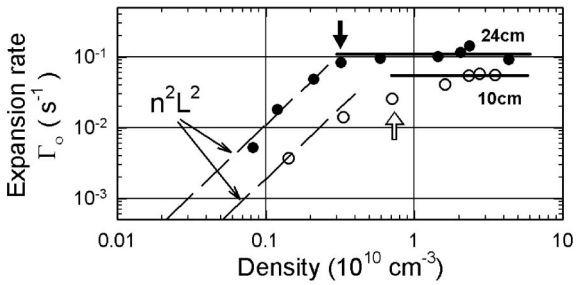

FIG. 5. Measured outward expansion rate after plasma compression (RW off) for two different plasma lengths. Arrows mark the densities where $\nu_{ee} = 3 f_b$, which appears to correspond with the transition to density independent transport.

$$P_H = \omega_{\mathrm{RW}} \mathcal{T}_{\mathrm{RW}} = \omega_{\mathrm{RW}} \frac{dL}{dt} = \omega_{\mathrm{RW}} L \Gamma_0, \qquad (1)$$

with L the total plasma angular momentum ($L \propto \sum r_j^2$, where r_j are the particle radii), and $\omega_{\mathrm{RW}} = 2\pi f_{\mathrm{RW}}$. Balancing this heating with the cyclotron cooling power, $P_c = N\Delta T \Gamma_c$, gives $\Delta T = T - T_W \approx 15$ meV, where T_W is the wall temperature, 25 meV. This estimate yields a steady-state temperature of $T \approx 40$ meV, which is a factor of $\sim$5 cooler than that observed. The higher plasma temperature is likely due to excess RW heating.

Previous experiments worked at a lower magnetic field and a larger transport rate [4], for which Eq. (1) predicts a factor of 10 higher temperature. This likely prevented achievement of the high-collisionality and strong-drive regimes reported here.

The steps observed in Fig. 4 appear to be due to a static asymmetry in the lab frame that drives a mode rotating opposite to the plasma, thereby producing a drag. Similar effects have been observed and studied previously in strongly coupled ion plasmas subject to laser torques [20]. The position and extent of these steps are consistent with low-order Trivelpiece-Gould modes [21], although we have been unable to make a definitive mode-number assignment.

In summary, we have discovered a new class of torque-balanced steady states of pure electron plasmas that can be accessed using strong RW drive and strong cyclotron cooling. Tuning to a plasma mode is not required. The limiting density corresponds to that at which the plasma rotation frequency is equal to the applied RW frequency. Plasmas can be compressed into a regime in which outward asymmetry-induced transport no longer increases rapidly with plasma density. The observed radial profiles and estimates of the thermal and momentum transport and heating rates indicate that these states are approximately uniform-temperature rigid rotors.

One important, but as yet unanswered, question is the maximum density that can be achieved using this technique. Since the observed transport does not increase rapidly with density in this regime, plasma heating will not be as much of a limiting factor as it would be in the regime where $\Gamma_0 \sim n^2$ [22].

The new regime reported here can be expected to be of considerable practical importance in tailoring antimatter (e.g., positron) plasmas for a range of applications, including the development of multicell traps for massive and long-term positron storage [22]. The plasmas studied here are nearly optimum for such devices. They can be confined and compressed without tuning to plasma modes, which facilitates multicell operation. In addition, the reduced transport in the high-density regime reduces plasma heating and, consequently, the requirements for plasma cooling.

This work is supported by NSF Grant No. PHY 03-54653. The high-field trap was built with ONR support. We thank J. P. Sullivan and P. Schmidt for their contributions to the design and construction of this device and E. A. Jerzewski for his expert technical assistance. We acknowledge numerous helpful conversations with F. Anderegg, C. F. Driscoll, R. W. Gould, R. G. Greaves, and T. M. O'Neil.

[1] C. M. Surko and R. Greaves, Phys. Plasmas **11**, 2333 (2004).
[2] *Non-neutral Plasma Physics V*, edited by M. Schauer, T. Mitchell, and R. Nebel (AIP Press, Melville, NY, 2003).
[3] F. Anderegg, E. M. Hollmann, and C. F. Driscoll, Phys. Rev. Lett. **81**, 4875 (1998).
[4] E. M. Hollmann, F. Anderegg, and C. F. Driscoll, Phys. Plasmas **7**, 2776 (2000).
[5] X.-P. Huang, F. Anderegg, E. M. Hollmann, C. F. Driscoll, and T. M. O'Neil, Phys. Rev. Lett. **78**, 875 (1997).
[6] X.-P. Huang, J. J. Bollinger, T. B. Mitchell, and W. M. Itano, Phys. Rev. Lett. **80**, 73 (1998).
[7] R. G. Greaves and C. M. Surko, Phys. Rev. Lett. **85**, 1883 (2000); Phys. Plasmas **8**, 1879 (2001).
[8] D. P. van der Werf *et al.*, in Ref. [2], p. 172.
[9] C. F. Driscoll and J. H. Malmberg, Phys. Rev. Lett. **50**, 167 (1983); C. F. Driscoll, K. S. Fine, and J. H. Malmberg, Phys. Fluids **29**, 2015 (1986).
[10] J. M. Kriesel and C. F. Driscoll, Phys. Rev. Lett. **85**, 2510 (2000).
[11] D. L. Eggleston and B. Carrillo, Phys. Plasmas **10**, 1308 (2003).
[12] D. H. Dubin and T. M. O'Neil, Rev. Mod. Phys. **71**, 87 (1999).
[13] D. L. Eggleston *et al.*, Phys. Fluids B **4**, 3432 (1992).
[14] B. R. Beck, J. Fajans, and J. H. Malmberg, Phys. Rev. Lett. **68**, 317 (1992).
[15] D. H. E. Dubin and T. M. O'Neil, Phys. Rev. Lett. **78**, 3868 (1997); E. M. Hollmann, F. Anderegg, and C. F. Driscoll, Phys. Plasmas **7**, 1767 (2000).
[16] T. M. O'Neil, Phys. Fluids **23**, 725 (1980).
[17] T. M. O'Neil, Phys. Fluids **26**, 2128 (1983).
[18] J. M. Kriesel and C. F. Driscoll, Phys. Rev. Lett. **87**, 135003 (2001).
[19] R. W. Gould, in *Non-Neutral Plasma Physics III*, edited by J. J. Bollinger, R. L. Spencer, and R. C. Davidson (American Institute of Physics, Melville, NY, 1999), p. 170.
[20] D. J. Heinzen, J. J. Bollinger, F. L. Moore, W. M. Itano, and D. J. Wineland, Phys. Rev. Lett. **66**, 2080 (1991).
[21] J. R. Danielson *et al.* (unpublished).
[22] C. M. Surko and R. G. Greaves, Radiat. Phys. Chem. **68**, 419 (2003).